Supporting Information

Nanoconfinement of Ultra-Small Bi_2Te_3 Nanocrystals on Reduced Graphene Oxide: A Pathway to High-Performance Sodium-Ion Battery Anodes

Zhuoying Cheng, Zhuo Li, Yuao Wang, Yiyang Mao, Jun Yan*, Dianxue Cao, Kai Zhu*

Key Laboratory of Superlight Materials and Surface Technology, Ministry of Education, College of Material Science and Chemical Engineering, Harbin Engineering University, Harbin 150001, China

*Corresponding authors.

E-mail: kzhu@hrbeu.edu.cn; yanjun198201@vip.163.com

Experimental

Materials and Chemicals: All the chemicals used in this work were of analytical grade and used as received without further purification. Graphite powders were purchased from Qingdao Graphite Company (Qingdao, China). Nitric acid (HNO_3), Ammonium chloride (NH_4Cl), Bismuth nitrate ($Bi(NO_3)_2 \cdot 5H_2O$) and Sodium tellurite (Na_2TeO_3) were obtained from Sinopharm Chemical Reagent Co. Ltd (China).

Preparation of the GO. GO was prepared by an improved Hummers method as described in the previous report [1].

Synthesis of Ultrasmall BiOCl/GO Composites. A nano-confinement strategy was employed to synthesize ultra-small BiOCl/GO composite materials. Typically, 0.9 mL of HNO_3 (0.01 M) solution was added to 30 mL of homogenized graphene oxide aqueous dispersion (0.2 mg mL^{-1}), and continuously stirred in an ice bath until the pH reached approximately 4. To this dispersion, 0.3 mL of $Bi(NO_3)_3 \cdot 5H_2O$ solution (0.5 M) was added, followed by 3 mL of NH_4Cl solution (0.2 M). The resulting precursor was continuously stirred in an ice bath for 5 min. The solution was then centrifuged and washed three times, and the obtained mixture was freeze-dried to obtain the BiOCl/GO aerogel.

Synthesis of Bi_2Te_3/GO composites. The pre-synthesized BiOCl/GO (2 mmol) was dispersed in 20 mL of deionized water and stirred magnetically for 20 minutes. Subsequently, 20 mL of Na_2TeO_3 solution (6 mmol) was added to the suspension and stirred magnetically for another 20 minutes. The mixture was transferred to a 100 mL Teflon-lined stainless-steel autoclave and subjected to hydrothermal treatment at

180°C for 24 hours. After naturally cooling to room temperature, the resulting precipitate was collected by filtration, washed multiple times with deionized water and ethanol to remove any residual impurities, and finally dried in air at 60°C for 12 hours. Pure Bi_2Te_3 was also synthesized by the same way but without the presence of GO.

Synthesis of Bi_2Te_3/rGO composites. For the synthesis of the ultrasmall Bi_2Te_3/rGO composites, The obtained Bi_2Te_3/GO was heated under N_2 to 350° C with a heating rate of 4° C/min and maintained at this temperature for 4 hours.

Materials characterization. The morphology of the materials was investigated by scanning electron microscope (SEM, Thermo Scientific, Apreo LoVac) and transmission electron microscope (TEM, FEI, Talos F200X G2). X-ray diffraction (XRD, Rigaku D/MAX-TTR III) equipped with Cu Kα radiation (λ =0.15406 nm) was used to determine the crystalline structures of the materials at a step of 0.02° with 0.24 s dwelling time. X-ray photoelectron spectroscopy (XPS) was tested by a Thermo Scientific Escalab Xi+ X-ray photoelectron spectrometer with a monochromated Al Kα X-ray source (1486.6 eV) and resolution of 0.80 eV at a working pressure lower than 10^{-8} mbar. The binding energy values were calibrated by referencing the C1s peak at 284.6 eV. Raman spectrum was acquired by a JY HR-800 Raman spectrometer with laser wavelength of 532 nm. Zeta potential analysis was tested by Malvern Zetasizer Nano ZS90. To measure the electrical conductivity, the powder samples were firstly pressed into pellets with diameters of 12 mm and then

measured using a four-point probe instrument (RM3000+, Jandel Engineering, UK) by repeating the test in at least 10 different positions.

SIB performance measurements. All electrochemical tests were conducted in CR2032 coin cells. For the preparation of anode, Bi_2Te_3/rGO composites (70 wt.%), Super P (Conductive carbon black, 20 wt.%) and polyvinylidene fluoride (PVDF 10 wt.%) were mixed in a mortar with nitromethyl pyrrolidone (NMP) as the solvent to make a homogeneous slurry, which was then uniformly coated onto a copper foil with a scraper and finally dried overnight at 80 ℃ in a vacuum oven. The mass loading of active material was 1.5 mg cm^{-2} in each electrode. Coin cells were assembled with sodium metal sheet as the counter and reference electrodes in an argon-filled glove box (H_2O and O_2 < 0.1 ppm). Porous polypropylene film (Celgard 2400) was used as the separator and 1 M $NaClO_4$ dissolved in a mixture of ethylene carbonate/dimethyl carbonate (EC/DMC, 1:1, v/v) was used as the electrolyte. All the electrode potential of the half-cells reported in this work is referred to the Na^+/Na reference electrode unless otherwise specified.

GCD tests were carried out on a NEWARE battery tester (CT-4008) in the voltage range of 0.005-3 V. CV measurements were performed on an electrochemical station (VMP3, Bio-Logic) within a potential window of 0.005-3 V. EIS were measured on a VMP3 electrochemical station with the AC amplitude of 5 mV in the frequency range of 100 kHz to 0.01 Hz. GITT measurements were carried out with current pulse (0.05 A g^{-1}) for 30 min followed by 60 min relaxation on a NEWARE battery tester (CT-4000). Li^+ diffusion coefficient could be calculated through the GITT method based on the following equation:

$$D = \frac{4}{\pi\tau}\left(\frac{m_B V_M}{M_B S}\right)^2\left(\frac{\Delta E_s}{\Delta E_\tau}\right)^2 \quad \text{(S2)}$$

where τ is the limited time period, m_B is the weight of active material, M_B is the relative molecular mass of active material, V_M is the molar volume, S is the contact area between electrode and electrolyte, ΔE_s is the steady potential difference in the plateau region, and ΔE_τ is the voltage drop between beginning state and steady state.

The diffusion coefficient (D) of Li^+ in the electrode can also be calculated as follows:[2]

$$D = \frac{R^2T^2}{2A^2n^4F^4C^2\sigma^2} \tag{S3}$$

$$Z' = R_s + R_{ct} + \sigma\omega^{-1/2} \tag{S4}$$

where R, T, A, n, F, C, σ, Z' and ω are the gas constant, absolute temperature, area of electrode/electrolyte interfaces, number of electron transferred, Faraday constant, concentration of OH^- ions, Warburg factor which could be obtained from the slope of the plot of Z' versus $\omega^{-1/2}$, real part of the complex impedance, and angular frequency, respectively.

Prior to the fabrication of full battery, the prelithiation of the Bi_2Te_3/rGO anode was performed to circumvent the large irreversible capacity and low ICE. For the preparation of the NVP cathode, the active material (80 wt.%), Super P (10 wt.%) and PVDF (10 wt.%) were mixed in a mortar with NMP as the solvent to make a homogeneous slurry, which was uniformly coated onto an aluminum foil with a scraper and finally dried overnight at 80 °C in a vacuum oven. 1 M $NaClO_4$ dissolved in a mixture of EC/DMC (1:1, v/v) was used as the electrolyte, and porous polypropylene film (Celgard 2400) was used as the separator. The mass ratio of cathode to anode was 2.1, which was determined based on the reversible capacity of the cathode and anode in the half cells with a N/P ratio of 1.1. The specific capacity of

the full battery was calculated based on the total mass of active materials of both the anode and cathode.

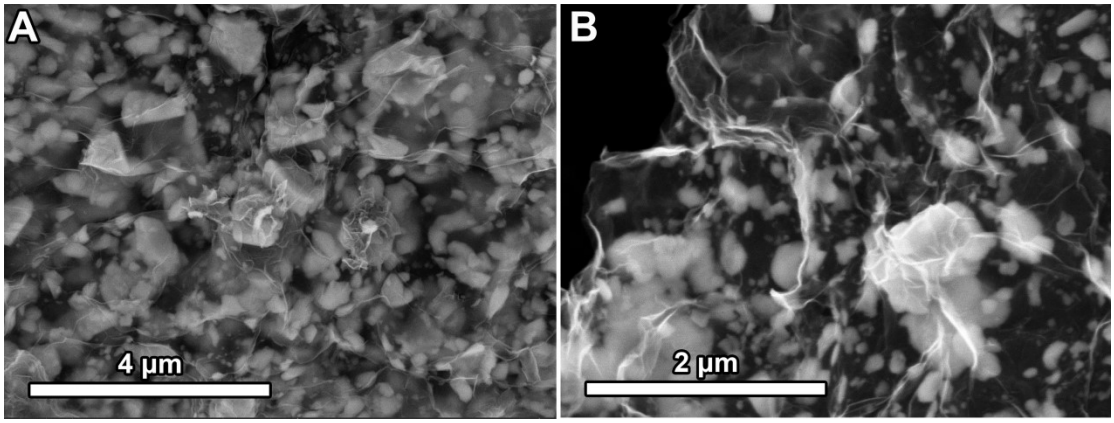

Figure S1. (A, B) SEM image of Bi_2Te_3/rGO.

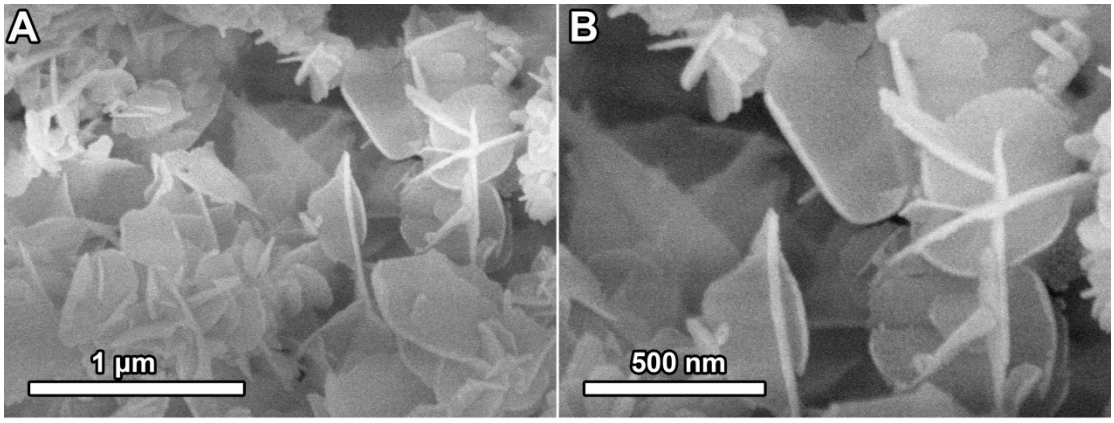

Figure S2. (A, B) SEM image of Bi_2Te_3.

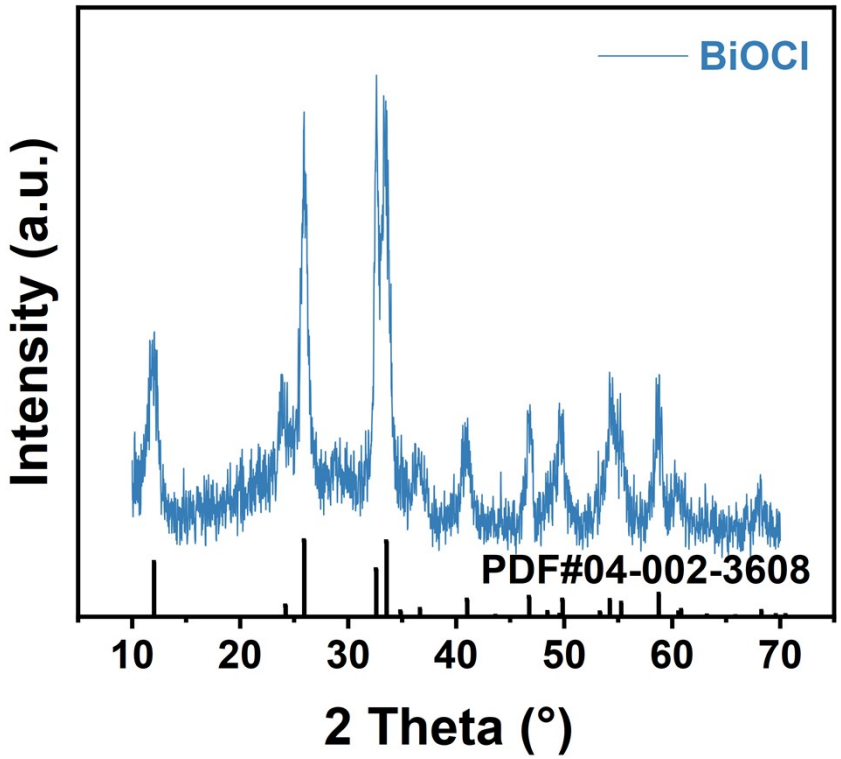

Figure S3. XRD pattern of BiOCl

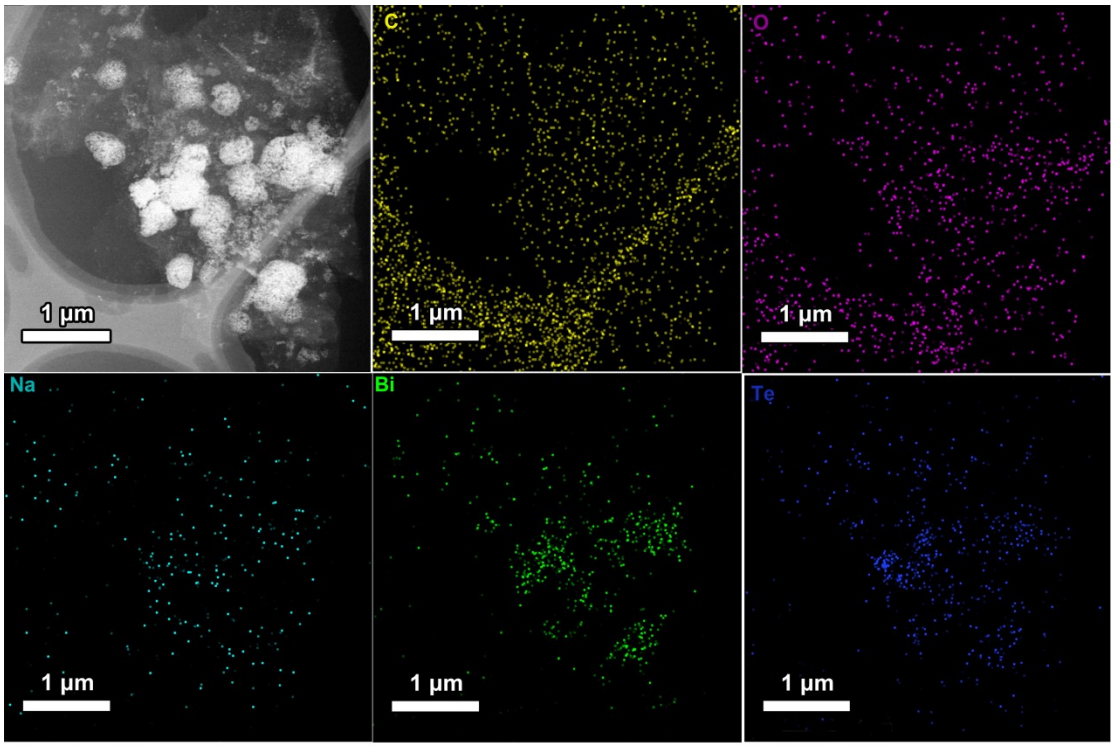

Figure S4. EDS elemental mapping images of the Bi_2Te_3/rGO electrode at discharge to 0.01V.

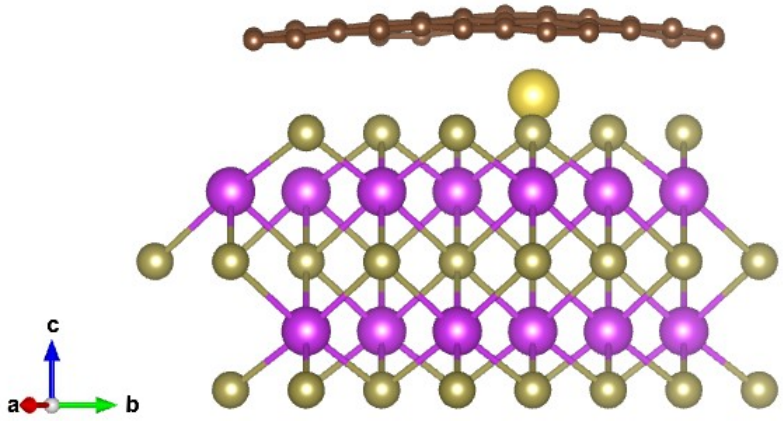

Figure S5. Calculation model of Bi_2Te_3/rGO.

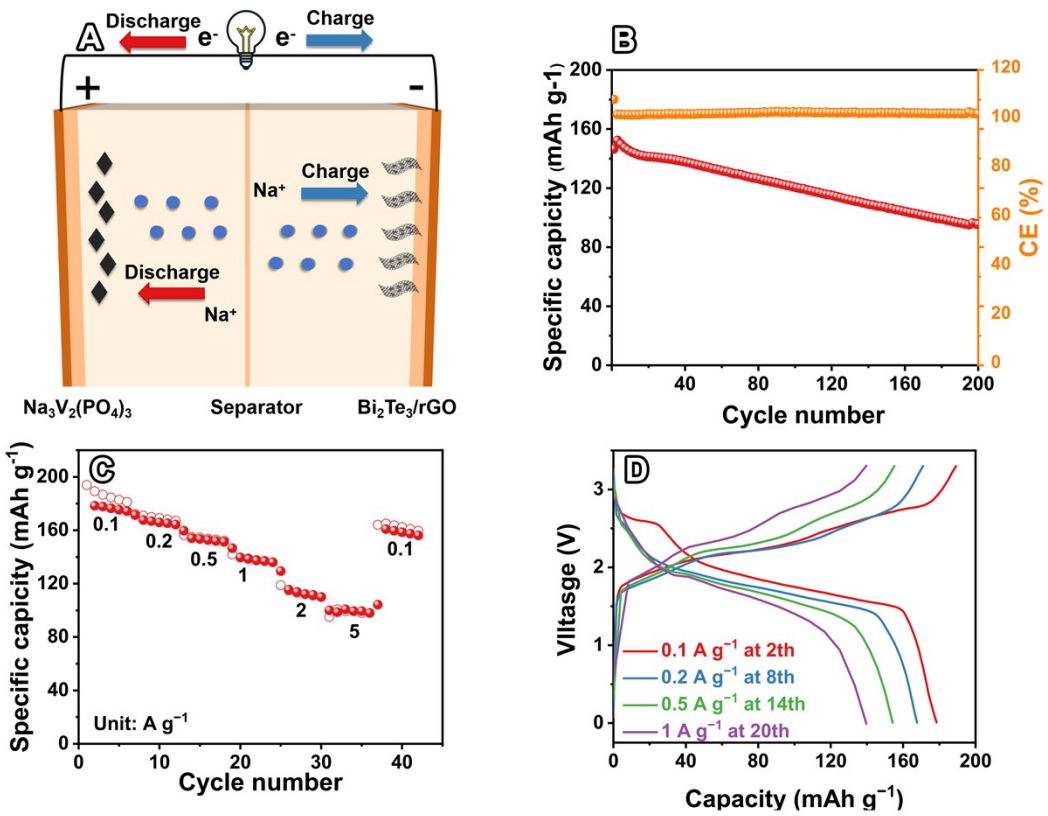

Figure S6. Electrochemical performances of our fabricated Bi_2Te_3/rGO// $Na_3V_2(PO_4)_3$ full cell. (A) Schematic illustration of the device. (B) GCD curves of the LFP and MNM-1 half cells at a current density of 0.1 A g-1. (C) GCD curves and (D) specific capacity at different current densities..

Table S1. Electrical conductivity of pristine Bi_2Te_3, Bi_2Te_3/rGO samples measured by four-point probe method.

Samples	Resistivity (Ω cm)	Conductivity (S cm^{-1})
Bi_2Te_3	295	0.33×10^{-2}
Bi_2Te_3/rGO	68	1.47×10^{-2}

Table S2. Fitting results of the Nyquist plots shown in Fig. 4E using the equivalent circuit.

Samples	Rs (Ω)	CPE (F)	Rct (Ω)	Zw (Ω $s^{-1/2}$)
Bi_2Te_3	5.14	9.8×10^{-5}	283	1604
Bi_2Te_3/rGO	0.88	4.9×10^{-6}	113.2	788

Table S3. Comparison of lithium storage performances of the Bi_2Te_3/rGO composite with those of the previously reported Bi_2Te_3 based materials.

Materials	Discharge capacity (mAh g^{-1}/A g^{-1})	Rate capacity (mAh g^{-1}/A g^{-1})	Ref.
Bi_2Te_3/rGO	**715/0.1**	**356/5**	**This work**
SnS/C	563/0.05	230/2	[2]
MoS_2/Fe_2O_3@ carbon fiber	406/0.2	167/5	[3]
MoSe2/rGO	567/0.1	287/10	[4]
MoS2/carbon dots	422/0.1	80/5	[5]
MoSe2	379/0.05	251/2	[6]
HC@MoS2@NC	413/0.2	249/10	[7]
$MoTe_2$/C	435/0.2	190/5	[8]
CoSe2-SnSe	370/0.1	160/1	[9]

References

1. Y. Zhang, P. Chen, Q. Wang, Q. Wang, K. Zhu, K. Ye, G. Wang, D. Cao, J. Yan and Q. Zhang, *Advanced Energy Materials*, 2021, **11**, 2101712.
2. J. Xia, L. Liu, S. Jamil, J. Xie, H. Yan, Y. Yuan, Y. Zhang, S. Nie, J. Pan, X. Wang and G. Cao, *Energy Storage Materials*, 2019, **17**, 1-11.
3. Q. Zhang, Y. Zeng, X. Chen, Y. Ding, H. Wang, L. Wang, H. Wang, X. Li, J. Xiao and T. Zhang, *Electrochim. Acta*, 2023, **470**, 143363.
4. Z. Li, L. Yu, X. Tao, Y. Li, L. Zhang, X. He, Y. Chen, S. Xiong, W. Hu, J. Li, J. Wang, H. Jin and S. Wang, *Small*, 2023, **n/a**, 2304124.
5. Y. Wang, Q. Wang, W. Liu, Y. Wei, S. Wang, S. Luo, Y. Zhang, P. Hou, S. Yan, X. Liu and J. Guo, *J. Colloid Interface Sci.*, 2024, **655**, 407-416.
6. N. Shi, G. Liu, B. Xi, X. An, C. Sun and S. Xiong, *Nano Res.*, 2023, DOI: 10.1007/s12274-023-6274-x.
7. G. Suo, B. Zhao, R. Mu, C. Lin, S. Javed, X. Hou, X. Ye, Y. Yang and L. Zhang, *Journal of Energy Storage*, 2024, **77**, 109801.
8. L. Zhang, J. Bai, Y. He, B. Lu, L. Xue, X. Kong and S. Guo, *J. Alloys Compd.*, 2023, **949**, 169884.
9. L. Gao, Y. Ma, C. Zhang and M. Cao, *Chem. Eng. Sci.*, 2024, **283**, 119390.